Biochemistry

pubs.acs.org/biochemistry Article

Bicarbonate-Mediated CO_2 Formation on Both Sides of Photosystem II

Dmitry Shevela,* Hoang-Nguyen Do, Andrea Fantuzzi, A. William Rutherford, and Johannes Messinger*

Cite This: *Biochemistry* 2020, 59, 2442–2449 Read Online

ACCESS | Metrics & More | Article Recommendations | Supporting Information

ABSTRACT: The effect of bicarbonate (HCO_3^-) on photosystem II (PSII) activity was discovered in the 1950s, but only recently have its molecular mechanisms begun to be clarified. Two chemical mechanisms have been proposed. One is for the electron-donor side, in which mobile HCO_3^- enhances and possibly regulates water oxidation by acting as proton acceptor, after which it dissociates into CO_2 and H_2O. The other is for the electron-acceptor side, in which (i) reduction of the Q_A quinone leads to the release of HCO_3^- from its binding site on the non-heme iron and (ii) the E_m potential of the $Q_A/Q_A^{\bullet-}$ couple increases when HCO_3^- dissociates. This suggested a protective/regulatory role of HCO_3^- as it is known that increasing the E_m of Q_A decreases the extent of back-reaction-associated photodamage. Here we demonstrate, using plant thylakoids, that time-resolved membrane-inlet mass spectrometry together with ^{13}C isotope labeling of HCO_3^- allows donor- and acceptor-side formation of CO_2 by PSII to be demonstrated and distinguished, which opens the door for future studies of the importance of both mechanisms under *in vivo* conditions.

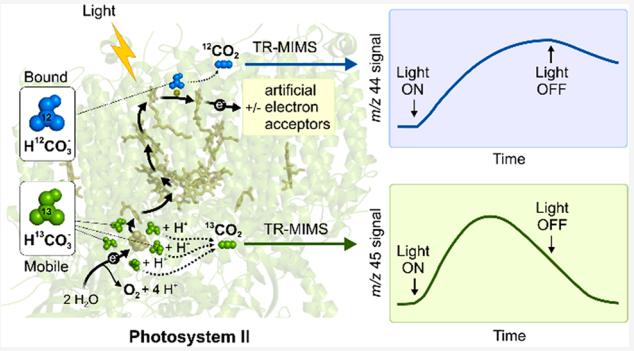

Photosynthetic organisms need atmospheric carbon dioxide (CO_2) as the terminal electron acceptor to store the captured energy of sunlight as energy-rich carbohydrates.[1,2] Cyanobacteria, algae, and higher plants also require CO_2 in solution in the form of bicarbonate ions (HCO_3^-), for the optimal function of photosystem II (PSII), the enzyme that catalyzes light-induced reduction of quinone and oxidation of water to molecular oxygen and protons.[3−6] The discovery of the "bicarbonate effect" on PSII activity in 1958[7] triggered a long-running debate about its role(s).[8,9] Two sites of interaction of HCO_3^- with PSII have been considered: one on the electron-donor side of PSII, where water oxidation takes place, and the other on the electron-acceptor side, associated with quinone reduction (Figure 1A).

It is now clear that HCO_3^- is not a tightly bound component of the oxygen-evolving complex and its catalytic site, the Mn_4CaO_5 cluster.[10−13] However, it was proposed that mobile, easily exchangeable HCO_3^- ions can stimulate water splitting by accepting protons produced by water splitting.[14−17] This action of HCO_3^- was proven experimentally by the direct detection of light-induced formation of O_2 and CO_2 by PSII using time-resolved membrane-inlet mass spectrometry (TR-MIMS).[18] This study also showed that the O_2 activity of PSII in HCO_3^--depleted media is reversibly reduced by ∼20%, likely *via* both donor- and acceptor-side (see below) effects of HCO_3^-. Moreover, a recent PSII mutagenesis study supports the role of HCO_3^- in the proton-egress pathway.[19] These observations led to the proposal that mobile HCO_3^- may contribute to a feedback mechanism that may adapt the availability of electrons for CO_2 reduction.[18]

On the acceptor side of PSII, HCO_3^- removal slows electron transfer through the quinone electron acceptors Q_A and Q_B.[20] This was subsequently rationalized by the discovery that HCO_3^- is a ligand of the non-heme iron (Fe^{2+}) (Figure 1A).[21−23] It was also suggested that HCO_3^- ions facilitate the protonation of Q_B.[24−26]

Given its reported binding constant and its concentration in the stroma, one HCO_3^- was thought to be permanently bound to the Fe^{2+}.[27,28] However, some earlier quantitative assays determined less than one HCO_3^- per PSII.[11,29,30] Our recent TR-MIMS study, carried out in the dark under air-saturated conditions, revealed exactly one HCO_3^- per PSII.[31] This unexpected variation was clarified recently, when it was shown that formation of $Q_A^{\bullet-}$ results in a weakening of HCO_3^- binding, which can lead to a release of HCO_3^- that in turn shifts the E_m of the $Q_A/Q_A^{\bullet-}$ couple by +74 mV.[32] The release of HCO_3^- was evidenced by the typical slowing of electron transfer from $Q_A^{\bullet-}$ to Q_B.[32] These results were interpreted as

Received: March 13, 2020
Revised: June 10, 2020
Published: June 23, 2020

https://dx.doi.org/10.1021/acs.biochem.0c00208
Biochemistry 2020, 59, 2442−2449

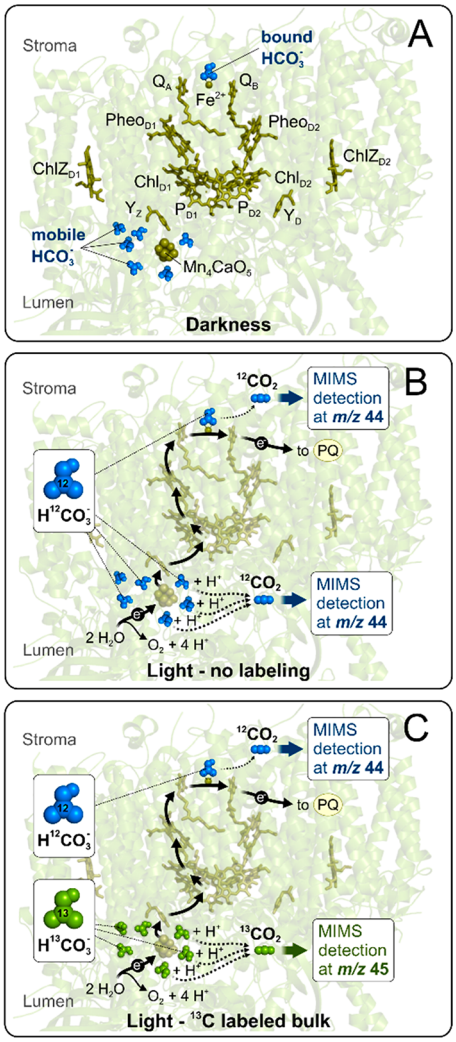

Figure 1. Redox-active cofactors and bicarbonate interactions in PSII. (A) Arrangement of redox-active cofactors and sites where bicarbonate (HCO_3^-) plays functional roles within PSII. One HCO_3^- molecule binds, in the dark, with high affinity to the Fe^{2+} between quinones Q_A and Q_B on the acceptor side of PSII, and this is resolved in the crystal structure;[13] mobile HCO_3^- molecules act as proton acceptors on the water-oxidizing side. Their locations are unknown but suggested to be in the proton exit channels[18] and thus have been placed there to illustrate that model. (B) Nonlabeling measuring conditions. Light-induced formation of CO_2 from HCO_3^- may occur as $^{12}CO_2$ on both sides of PSII. Thus, all released CO_2 should be detected by TR-MIMS at m/z 44. (C) Labeling of the medium with $H^{13}CO_3^-$. $^{13}CO_2$ formation is expected (m/z 45) from light-induced water splitting leading to the protonation of mobile $H^{13}CO_3^-$ (Figure 2 and Figure S1), while the release of slowly exchangeable (in darkness with a low CO_2/HCO_3^- content) $H^{12}CO_3^-$ from its binding site at the Fe^{2+} would generate $^{12}CO_2$ (m/z 44) (Figure S2). The structure of PSII was generated using Protein Data Bank entry 3ARC.[13]

providing a mechanism by which the PSII activity is regulated by the ambient HCO_3^-, and hence by CO_2, and by the redox state of Q_A.[32] In this case, the upshift in the E_m of the $Q_A/Q_A^{\bullet-}$ couple upon the release of HCO_3^- increases the energy gap between $Q_A^{\bullet-}$ and pheophytin $(Pheo)_{D1}$, disfavoring the back-reaction route that is known to generate the radical-pair recombination chlorophyll (Chl) triplet state[33] and hence singlet oxygen.[34] The acceptor-side redox tuning mechanism is thus not only regulatory but also protective.[32] The aspect of protection is crucial, as simply slowing PSII electron transfer when CO_2, the terminal acceptor, is limiting is likely to result in an increased level of photodamage unless a protective mechanism is also triggered.

The acceptor-side regulation may be modulated by the binding of other carboxylic acids.[32] This proposal was supported by reports that acetate in the growth medium appears to displace HCO_3^- from the acceptor side of PSII in *Chlamydomonas*.[35] A similar effect was seen in a photorespiration mutant of *Arabidopsis* in which high concentrations of glycolate accumulated.[36] However, despite the observations mentioned above, no direct experimental evidence for light-induced evolution of CO_2 from the non-heme Fe^{2+} has been reported.

In the study presented here, we refined the TR-MIMS experiments to probe selectively for the light-induced production of CO_2 at the acceptor and donor sides of PSII (Figure 1B). For this, we employed $H^{13}CO_3^-$ labeling of the thylakoid suspension (Figure 1C) and modulated the oxidation state of the acceptor-side quinones by using varying concentrations of exogenous electron acceptors. The MIMS signals obtained clearly demonstrate that both the HCO_3^- bound at the Fe^{2+} on the PSII acceptor side and mobile HCO_3^- molecules protonated within PSII during water splitting contribute to light-induced CO_2 formation by PSII.

MATERIALS AND METHODS

Chemicals and Reagents. $NaH^{13}CO_3$ (99% ^{13}C), $NaH^{12}CO_3$ (>99.7%), 2-phenyl-*p*-benzoquinone (PPBQ, >95%), and potassium ferricyanide, $K_3[Fe(CN)_6]$ (>99.99%), were purchased from Sigma-Aldrich. All [$^{12}C/^{13}C$]bicarbonate stock solutions were prepared shortly before the experiments in deionized and filtered (Milli-Q) water depleted of inorganic carbon (C_i). Depletion of C_i in water was carried out as described earlier by intensive flushing with nitrogen in septum-sealed vials for 20−30 min.[16] To avoid contamination with atmospheric CO_2, the C_i-depleted water was added to the weighed batches of $NaH^{13}CO_3/NaH^{12}CO_3$ inside a glovebox (OMNI-Lab System, VAC, Hawthorne, CA) under a N_2 atmosphere. The resulting stock solutions of $NaH^{13}CO_3$ and $NaH^{12}CO_3$ (30 mM each) were kept in septum-sealed vials until they were used. PPBQ (50 mM) and $K_3[Fe(CN)_6]$ (100 mM) stock solutions were freshly prepared in DMSO (>99.9%) and in Milli-Q water, respectively.

Sample Preparations. Isolated thylakoids were prepared from fresh leaves of *Spinacia oleracea* as described previously.[37,38] After being isolated, the thylakoids were frozen in liquid N_2 in small aliquots (in sucrose buffer containing 400 mM sucrose, 5 mM $CaCl_2$, 5 mM $MgCl_2$, 15 mM NaCl, and 50 mM MES/NaOH adjusted to pH 6.0 and at [Chl] = ∼2 mg mL^{-1}) and stored at −80 °C until they were used. Control rates of O_2 evolution for our thylakoid preparations were ∼180−200 μmol of O_2 (mg of Chl)$^{-1}$ h^{-1} [as measured by a Clark-type electrode at 20 °C using continuous saturating light (∼1500 μmol of photons m^{-2} s^{-1}) in the presence of 0.25 mM PPBQ and 0.5 mM $K_3[Fe(CN)_6]$ as artificial electron acceptors]. Shortly before the measurements, the samples were thawed in the dark on ice, washed once in MES medium (containing 15 mM NaCl, 5 mM $CaCl_2$, 5 mM $MgCl_2$, and 3 mM MES/NaOH adjusted to pH 6.39), and diluted to the desired Chl concentrations (see below). This MES medium was used in all of the MIMS experiments described herein. A

https://dx.doi.org/10.1021/acs.biochem.0c00208
Biochemistry 2020, 59, 2442−2449

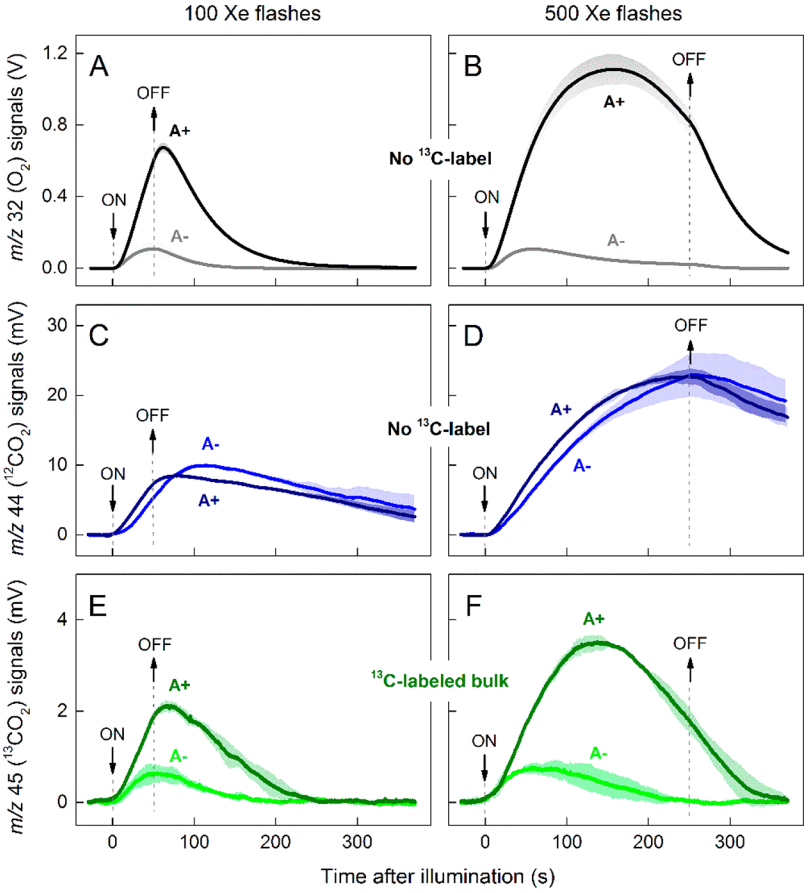

Figure 2. Online TR-MIMS measurements of the production of O_2 and CO_2 by spinach thylakoids. Dark-adapted thylakoids (0.5 mg of Chl mL^{-1}) were illuminated with 100 (panels A, C, and E) or 500 (panels B, D, and F) xenon flashes (at 2 Hz) in the absence (A− traces) or presence (A+ traces) of artificial electron acceptors {0.25 mM PPBQ and 0.5 mM $K_3[Fe(CN)_6]$}. Traces of O_2 (A and B) and $^{12}CO_2$ (C and D) evolution were measured simultaneously at m/z 32 and 44, respectively, after the addition of 1 mM $NaH^{12}CO_3$ and subsequent sample degassing for 20−30 min to reach a stable baseline. Traces of $^{13}CO_2$ (E and F) evolution were obtained at m/z 45 after the addition of 1 mM $NaH^{13}CO_3$ and subsequent degassing of thylakoid preparations inside the MIMS cell for 20−30 min. The measurements were performed in MES medium (3 mM MES at pH 6.39) at 20 °C. The arrows indicate the start and end of the train of flashes. Zero levels are offset for the sake of clarity of presentation. In all panels, the means (solid traces) of two to three repeats and standard errors (shaded areas) are presented.

sufficiently low concentration of MES in this medium was needed to minimize the competition of MES with HCO_3^- in proton removal from the water-splitting site of PSII while still allowing it to buffer the pH of the medium.[18]

Online TR-MIMS Assays and $H^{13}CO_3^-$ Labeling. Our TR-MIMS setup[39,40] consisted of an isotope ratio mass spectrometer (Finnigan DELTA^{plus}XP, Thermo, Bremen, Germany) connected *via* a cold trap (dry ice/ethanol) to a 150 μL in-house-constructed membrane-inlet cell described previously.[18] The sample volume of the cell was isolated from the vacuum (3×10^{-8} mbar) of the mass spectrometer by a gas-permeable silicon membrane (25 μm thick; type MEM-213, MemPro, Troy, NY) that was supported by a porous Teflon disc (Ø 1 cm; Small Parts Inc., Miami Lakes, FL). Thylakoids diluted with MES medium (see above) were injected into the MIMS cell to a final concentration of 0.5 mg of Chl mL^{-1}. If not stated otherwise, the sample suspension also contained 0.25 mM PPBQ and 0.5 mM $K_3[Fe(CN)_6]$ as an exogenous electron-acceptor system. All of these manipulations were performed under dim green light. During the assays, the MIMS cell was thermostated at 20 °C and the sample suspension was constantly stirred at high speed (1000 rpm) with a magnetic stir bar. After the sample suspension had been loaded into the MIMS cell, the samples were thoroughly degassed in the dark for ∼40 min by the vacuum pump of the mass spectrometer. After degassing, the bulk medium of the sample suspension was labeled with ^{13}C by injection of 5 μL of $NaH^{13}CO_3$ into the MIMS cell to a final concentration of 1 mM. For control experiments, the same amount of $NaH^{12}CO_3$ was injected into the MIMS cell. All transfers and injections of bicarbonate solutions were performed with gastight Hamilton syringes that had been preflushed with nitrogen. After addition of the [$^{13}C/^{12}C$]bicarbonate solutions, the sample suspensions were incubated and stirred for approximately 20−30 min. This time was enough to reach stable and identical baseline values for $^{12}CO_2/^{13}CO_2$ and to equilibrate the ^{13}C label between the remaining C_i species in the aqueous fraction of the sample. Light-induced evolution of gases (O_2 and $^{13}CO_2/^{12}CO_2$) was monitored upon illumination of the thylakoids with a train of 100 or 500 short (∼5 μs full width at half-maximum) saturating flashes (2 Hz) given by a xenon flash lamp (model FX-4400, Excelitas Technologies Illumination, Inc., Salem, MA). O_2 and nonlabeled CO_2 evolved by thylakoids were detected simultaneously at m/z 32 and 44, respectively, with the same sensitivity of Faraday Cups (Figure 1B). In the ^{13}C labeling experiments (Figure 1C), $^{13}CO_2$ evolution was monitored at m/z 45 using the same Faraday Cup as for detection of $^{12}CO_2$ m/z 44 signals (Figures S1 and S2). This

https://dx.doi.org/10.1021/acs.biochem.0c00208
Biochemistry 2020, 59, 2442−2449

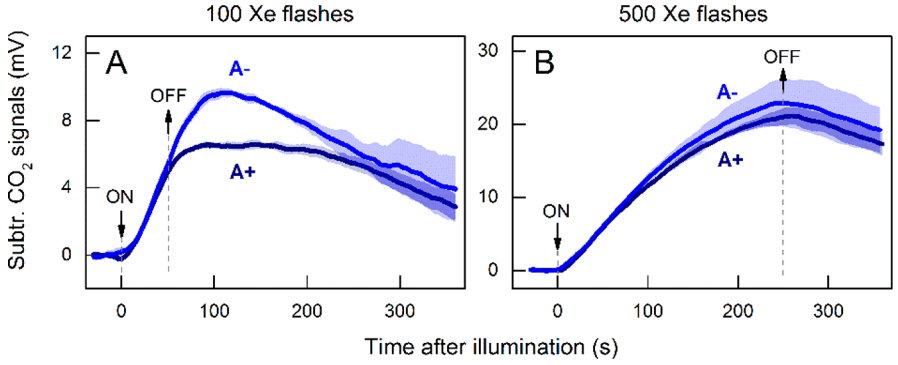

Figure 3. Resulting TR-MIMS CO_2 signals upon subtraction of m/z 45 curves (Figure 2E,F) from corresponding m/z 44 traces (Figure 2C,D) obtained after illumination with (A) 100 and (B) 500 Xe flashes. For other conditions, see Figure 2 and Materials and Methods.

allowed us to obtain $^{13}CO_2$-MIMS signals with the same sensitivity and selectivity as for the $^{12}CO_2$-MIMS signals.

RESULTS

Light-induced O_2 [m/z 32 (Figure 2A,B)] and $^{12}CO_2$ [m/z 44 (Figure 2C,D)] evolution by spinach thylakoids was monitored using TR-MIMS in nonlabeled bulk medium. The experiments were performed in the presence or absence (labeled A+ or A−, respectively) of the artificial electron-acceptor system (0.25 mM PPBQ and 0.5 mM potassium ferricyanide). Gas evolution was monitored upon illumination with 100 (Figure 2A,C) and 500 saturating xenon flashes (Figure 2B,D).

In the absence of exogenous electron acceptors, the total O_2 yield (gray traces in panels A and B of Figure 2) was equally small irrespective of the application of 100 or 500 flashes. This is simply a reflection of the limited number of enzyme turnovers possible with the small intrinsic electron-acceptor pool.

As expected, the level of O_2 production was much higher in the presence of electron acceptors (black lines in panels A and B of Figure 2). However, Figure 2B (black trace) shows that the O_2 evolution reached a plateau at ∼300 flashes and decreased thereafter. Because the concentration of the artificial electron acceptors was adjusted to be just enough for 500 flashes (for details, see the Supporting Information), we propose that the decline in O_2 production is due to the limited acceptor pool size and possibly some photodamage.

For 100 flashes in the presence of the electron acceptors (Figure 2A, black trace), the trace looks different compared to the trace obtained in the absence of the acceptors (Figure 2A, gray trace). Here, the O_2 yield continued to increase for ∼7 s in the dark after the flash train ended, reaching a maximum before falling back to the original level ∼200 s after the flash train. The increase in the rate of release of O_2 immediately after the end of the flash train reflects the instrument response time, which is also observed for all traces as an apparent lag in O_2 evolution at the onset of illumination. The decrease in the O_2 concentration after the flash train is due to the pervaporation of the dissolved O_2 through the silicon membrane into the high vacuum of the mass spectrometer.[40]

Panels C and D of Figure 2 show the kinetics of $^{12}CO_2$ evolution when monitored simultaneously with O_2 concentration. This experiment is sensitive to $^{12}CO_2$ released by both mechanisms: (i) from the donor side, where mobile $H^{12}CO_3^-$ reacts with protons generated by water oxidation to form CO_2 and H_2O,[18] and (ii) from the acceptor side, where the bound $H^{12}CO_3^-$ is released from its site at the non-heme Fe^{2+} during illumination,[31] after which it may also dissociate into CO_2 and H_2O after protonation. In contrast to O_2 evolution (Figure 2A,B), the $^{12}CO_2$ evolution traces (Figure 2C,D) were much less dependent on the presence of the exogenous electron acceptors; in fact, a similar quantity of CO_2 was formed with and without the added electron-acceptor system. Nevertheless, the presence of the electron acceptors did result in CO_2 release occurring more rapidly than in the absence of acceptors, and this was the case whether 100 or 500 flashes were used. This more rapid increase in the level of CO_2 when electron acceptors were present (Figure 2C,D, dark blue traces) appears to correspond to the rapid increase in the level of O_2 evolution (Figure 2A,B, black traces), and this part of CO_2 release can thus be attributed to the donor-side mechanism (see also below).

The kinetics for $^{12}CO_2$ evolution in the absence of an exogenous electron acceptors (Figure 2C,D, bright blue traces) is noticeably slower than the diffusional step for O_2 detection (Figure 1A, black trace), and we thus associate this slower phase with CO_2 formation at the acceptor side. The slow kinetics for the onset of CO_2 production could reflect (i) the loss of long-lived $Q_A^{\bullet-}$ under these conditions due to charge recombination with the donor side, (ii) the slow release of HCO_3^- when $Q_A^{\bullet-}$ is present,[32] or (iii) the slow conversion of the released HCO_3^- to CO_2 at this pH (see below). In comparison to O_2 evolution, the CO_2 release measured in the absence of electron acceptors also continued for much longer after the end of the flash train (compare panels C and D of Figure 2 with panels A and B of Figure 2). In Figure 2C, after the 100 flashes were given, at 50 s during the time course, the amount of CO_2 continues to increase in the dark for a further ∼50 s. The lengthy phase of CO_2 emission in the dark after the cessation of illumination could reflect the second and (more likely) the third of the three options discussed above.

When 500 flashes were given (Figure 2D), the amount of CO_2 released in the sample lacking the exogenous electron acceptors increased with flash number, but the slope decreases toward the end of the flash train. Given the absence of any CO_2 originating from the donor side at this time under these conditions, due to the lack of O_2 production, the $^{12}CO_2$ released (Figure 2D, bright blue trace) can be assigned as arising purely from the gradual release of the bound acceptor-side bicarbonate, which appears to be nearly complete at this time point.

The two kinetic components in the data in panels C and D of Figure 2 thus demonstrate the presence of two sources for CO_2 formation, which we assign to the donor side and

https://dx.doi.org/10.1021/acs.biochem.0c00208
Biochemistry 2020, 59, 2442−2449

acceptor side, respectively. This is in line with our previous MIMS measurements showing CO_2 production on the donor side, where HCO_3^- was thought to act as a proton acceptor during water oxidation, and our recent electrochemical and fluorescence data providing strong evidence that indicated the release of HCO_3^- from the non-heme iron when $Q_A^{\bullet-}$ was present for a prolonged period of time.[18,32] The data in Figures 2 and 3 also show that acceptor-side CO_2 formation is dominant under the experimental conditions used, which entail a low availability of HCO_3^- in the medium, thus largely suppressing CO_2 production at the donor side. The low HCO_3^- concentration additionally promotes the release of HCO_3^- from the acceptor side.

To confirm this assignment further and to selectively record the evolution of CO_2 from the electron-donor side, we added $H^{13}CO_3^-$ to the bulk medium. This approach is based on the assumption that $H^{12}CO_3^-$ bound to the non-heme iron does not significantly exchange with $H^{13}CO_3^-$ within the 20−30 min incubation time after its addition to the medium. This assumption appears to be reasonable given that (i) HCO_3^- binds in the dark tight enough to the non-heme iron to allow only slow dissociation into the medium, even at low external HCO_3^- concentrations, and (ii) the binding to empty sites at the non-heme iron competes with the consumption by the mass spectrometer.[31,32] In contrast, HCO_3^- acting as a proton acceptor at the donor side can be easily removed and thus exchangeable.[18]

Light-induced $^{13}CO_2$, monitored at m/z 45 (Figure 2E,F), occurred with kinetics and relative amplitudes that closely resembled those of O_2 evolution under the various conditions, albeit at much smaller absolute amplitudes. While the present setup does not allow for calibration of the signals, we estimate the $^{13}CO_2/O_2$ ratio to be on the order of 0.3−1.3% on the basis of the relative signal amplitudes and amplification factors (this estimate neglects differences in ionization efficiencies).[18] The excellent kinetic match between the O_2 and $^{13}CO_2$ release data thus provides strong support for the assumptions made above and the assignment of the fast phase of CO_2 evolution observed in panels C and D of Figure 2 in the presence of electron acceptors to mobile bicarbonate acting as a proton acceptor during water splitting.[18]

Taking into account the fact that m/z 44 and 45 signals (panels C and D and panels E and F, respectively, of Figure 2) were recorded with identical sensitivity and selectivity (because both were monitored by the same Faraday cup), it is clear that the donor-side CO_2 release is slower than acceptor-side release, as already suggested above by the unlabeled data (Figure 2C,D). To obtain pure kinetics for acceptor-side CO_2 formation, we subtracted the corresponding curves in Figure 2C−F (Figure 3). In principle, this difference signal may reflect one HCO_3^- per PSII reaction center after 500 flashes where the acceptor-side release appears to be nearly complete (see above). However, under the conditions of the TR-MIMS experiment with the degassing procedures used, we estimate the occupancy of bicarbonate at the non-heme iron site to be 0.3−0.5 HCO_3^- per PSII.[11]

Surprisingly, acceptor-side CO_2 formation is nearly identical for samples with and without the acceptor during the flash train, as seen from the same initial slopes for CO_2 formation in Figure 3. However, after the train of 100 flashes, there is marked difference comparing the traces obtained with and without the acceptor. This difference is less marked in the data from the experiments using 500 flashes, reflecting the nearly complete release of HCO_3^- during the flash train under both experimental conditions.

DISCUSSION

The results of this study provide strong evidence of two separate mechanisms of light-induced CO_2 formation by PSII, one involving mobile (bulk) HCO_3^- and one firmly bound (slowly exchangeable) HCO_3^-. We assign the slower kinetics to CO_2 formation at the electron-acceptor side of PSII, where HCO_3^- bound to the Fe^{2+} is released into the medium under illumination, and in the absence of added electron acceptors also for extended times in the dark after the end of the illumination. While some open questions remain (see below), the data overall support the idea that this CO_2 formation is due to the reduction of the endogenous electron acceptors of PSII, in agreement with the earlier correlation of formation of $Q_A^{\bullet-}$ with bicarbonate release.[32] We assign the faster phase of CO_2 formation to the electron-donor side, where mobile HCO_3^- accepts protons produced by the Mn_4CaO_5 cluster during light-induced water splitting, presumably within the channels of PSII, and then decomposes into H_2O and CO_2.[18]

The donor-side release of CO_2 correlates closely with O_2 evolution in terms of both its rate and its relative extent. The absolute extent of CO_2 release is small (≈1% of the O_2 yield) in this work because of the low level of free bicarbonate left in the experimental buffer after the extensive degassing that was required to allow the experiments to be performed. The CO_2 yield is further reduced by the competition for protons between HCO_3^- and MES molecules in the medium.[18] Experiments in intact cells or chloroplasts will be required to determine the magnitude and functional importance of the donor-side CO_2 evolution under *in vivo* conditions.

The CO_2 attributed to the HCO_3^- released from the acceptor side of PSII was observed when thylakoids were illuminated, supporting the hypothesis that reduced quinones decrease the binding affinity of HCO_3^- at the non-heme iron. However, we did not find the expected clear difference during the flash train with and without the added electron-acceptor mix. However, a clear difference was seen in the dark after the series of 100 flashes. In the absence of the electron-acceptor system, the CO_2 concentration continued to increase in the dark after the flash train, while when the acceptor system was present, the post-illumination increase in the level of CO_2 was much less marked. When the acceptor system was absent, 100 flashes was more than enough to reduce Q_A (by one electron), Q_B (by two electrons), and the plastoquinone (PQ) pool (a capacity of 14 electrons when taken as seven PQs). The significant quantity of CO_2 released in the dark after the flash train could reflect (i) the presence of $Q_A^{\bullet-}$, which is known to trigger HCO_3^- release,[32] and (ii) the presence of other reduced forms of quinone, $Q_B^{\bullet-}/Q_BH_2$, and the fully reduced PQH_2 pool, all of which can equilibrate with $Q_A^{\bullet-}$ and could result in bicarbonate dissociation. It is also possible that bicarbonate binding may be weakened by the physical presence of reduced quinones in the Q_B site (i.e., $Q_B^{\bullet-}$ or Q_BH_2). We note that an additional complexity arises from the fact that both PPBQ and $K_3[Fe(CN)_6]$ can oxidize the non-heme Fe^{2+} to Fe^{3+} in some of the centers. While $K_3[Fe(CN)_6]$ may do so in a fraction of the centers during the dark time before the flash train, PPBQ is known to oxidize the non-heme iron on odd-numbered flashes by a mechanism known as reductant-induced oxidation.[41] However, the presence of the $K_3[Fe(CN)_6]$ is likely to compete for the semiquinone that oxidizes the Fe^{2+}.

https://dx.doi.org/10.1021/acs.biochem.0c00208
Biochemistry 2020, 59, 2442−2449

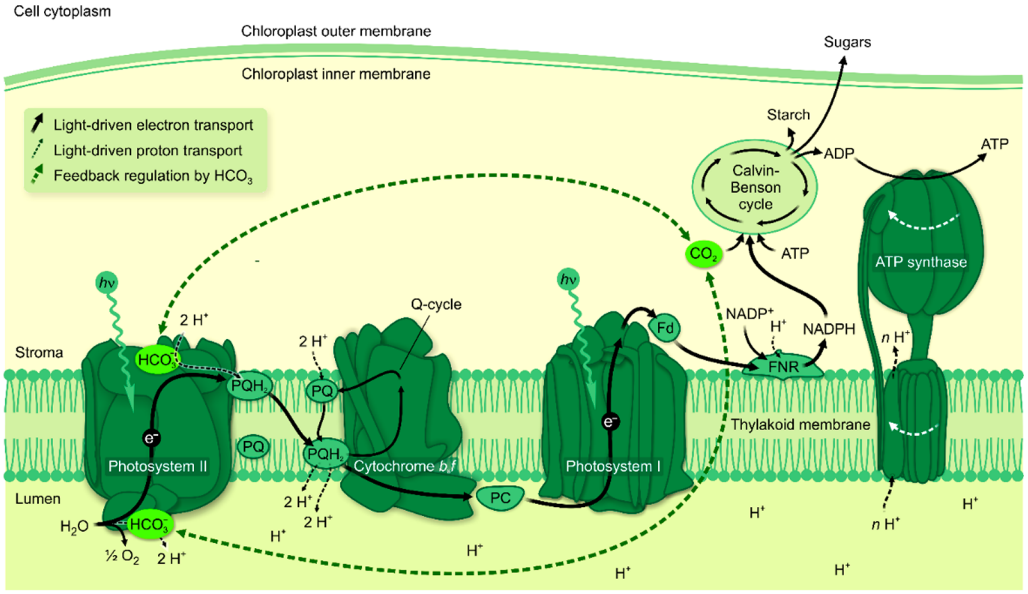

Figure 4. Possible regulation sites of oxygenic photosynthesis by inorganic carbon. Abbreviations of the components involved in electron transfer: PQ, plastoquinone; PQH_2, plastoquinol; PC, plastocyanin; Fd, ferredoxin; FNR, ferredoxin-NADP reductase.

While we might expect Fe^{3+} to bind bicarbonate more tightly than Fe^{2+}, this is likely affected by the proton release that accompanies the oxidation of the iron, and a bidentate/monodentate ligation difference could also affect the binding properties upon the Fe^{2+} to Fe^{3+} oxidation step.[22] This aspect will require more detailed attention in the future.

The absence of a post-100 flash CO_2 release with an added electron acceptor could be due to the remaining PPBQ/$K_3[Fe(CN)_6]$ acceptor system removing any electrons from the intrinsic acceptors. This would mean that the binding of the bicarbonate would revert to being tight due to the absence of reduced intrinsic quinone acceptors.

The unexpected observation that bicarbonate (in the form of CO_2) is also released upon illumination when the exogenous electron acceptors are present could at least partially be due to the low concentration of free bicarbonate ions in solution under the conditions needed for the experiments. The low concentration of bicarbonate would decrease the rate at which bicarbonate would bind to the non-heme iron. Consequently, the rate of bicarbonate dissociation could become competitive with the electron transfer kinetics of the forward reaction, $Q_A^{\bullet-}$ to Q_B, and/or the back-reactions, $Q_B^{\bullet-}$ to Q_A and Q_BH_2 to Q_A. This view is supported by MIMS experiments at a higher level of residual HCO_3^- in the medium (see Figure S3), in which acceptor-side CO_2 formation was not observed after the end of the flash train in samples containing no added acceptor. Further experiments combining TR-MIMS with simultaneous fluorescence measurements are required to fully resolve the details of the light-induced release of HCO_3^- from the electron-acceptor side.

CONCLUSIONS

The direct measurement of light-induced CO_2 formation at the acceptor side of PSII reported here using TR-MIMS complements the less direct demonstrations of the release of HCO_3^- from the non-heme Fe reported previously, i.e., (i) the light-induced shift in the redox potential of the $Q_A/Q_A^{\bullet-}$ couple to a value typical of bicarbonate-depleted PSII and (ii) the light-induced shift in the kinetics of $Q_A^{\bullet-}$ oxidation to a slower rate typical of bicarbonate-depleted PSII and its recovery by re-addition of bicarbonate.[32] In addition, our data demonstrate a second kinetic phase of release of CO_2 that closely correlates with O_2 evolution and thus is assigned to HCO_3^- acting as a proton acceptor during water oxidation.

The donor- and acceptor-side effects may both be rationalized in terms of regulatory mechanisms in which the terminal electron acceptor, CO_2, in the form of HCO_3^-, influences PSII function (Figure 4).[18,32] Decreased concentrations of CO_2 will result in decreased concentrations of HCO_3^- ions, which will have an immediate effect on the donor-side function if no other proton acceptors are present. On the other hand, this will initially have little effect on the acceptor side as the bicarbonate is strongly bound under normal functional conditions. However, once the electron-acceptor side becomes reduced, as it would when the PQ pool is reduced when CO_2 fixation becomes limiting (Figure 4), the affinity for bicarbonate would decrease, leading to its release. The release of HCO_3^- slows Q_BH_2/PQ exchange and also results in a positive shift in the E_m of the $Q_A/Q_A^{\bullet-}$ couple, and this increases the energy gap between Q_A and $Pheo_{D1}$, disfavoring the Chl triplet-mediated, singlet O_2-generating, back-reaction route that gives rise to photodamage.[32,34]

Although indications have been reported that bicarbonate effects are present in plants and cells of green algae,[35,36,42−44] further experiments with simultaneous TR-MIMS and fluorescence assays are required to determine the mechanistic aspects and the importance of HCO_3^-/CO_2-mediated feedback regulation at the donor and acceptor sides of PSII *in vivo*.

ASSOCIATED CONTENT

Supporting Information

The Supporting Information is available free of charge at https://pubs.acs.org/doi/10.1021/acs.biochem.0c00208.

Supplementary data (Figures S1−S3) and Methods (PDF)

https://dx.doi.org/10.1021/acs.biochem.0c00208
Biochemistry 2020, 59, 2442−2449

Accession Codes

UniProt IDs: *S. oleracea* PsbA, P69560; *S. oleracea* PsbD, P06005.

AUTHOR INFORMATION

Corresponding Authors

Dmitry Shevela − *Department of Chemistry, Chemical Biological Centre, Umeå University, 90187 Umeå, Sweden;* orcid.org/0000-0002-5174-083X; Phone: +46-90-786-5293; Email: dmitry.shevela@umu.se

Johannes Messinger − *Department of Chemistry, Chemical Biological Centre, Umeå University, 90187 Umeå, Sweden; Molecular Biomimetics, Department of Chemistry-Ångström Laboratory, Uppsala University, 75120 Uppsala, Sweden;* orcid.org/0000-0003-2790-7721; Phone: +46-18-471-3671; Email: johannes.messinger@kemi.uu.se

Authors

Hoang-Nguyen Do − *Department of Chemistry, Chemical Biological Centre, Umeå University, 90187 Umeå, Sweden*

Andrea Fantuzzi − *Department of Life Sciences, Imperial College London, London SW7 2AZ, United Kingdom*

A. William Rutherford − *Department of Life Sciences, Imperial College London, London SW7 2AZ, United Kingdom*

Complete contact information is available at: https://pubs.acs.org/10.1021/acs.biochem.0c00208

Funding

This work was supported by Vetenskapsrådet (2016-05183 to J.M.) and by Biotechnology and Biological Sciences Research Council (BBSRC) Grants BB/K002627/1 and BB/R00921X/ to A.W.R. and A.F.

Notes

The authors declare no competing financial interest.

ABBREVIATIONS

Chl, chlorophyll; Fe^{2+}, non-heme iron; MES, 2-(*N*-morpholino)ethanesulfonic acid; PPBQ, 2-phenyl-*p*-benzoquinone; Pheo, pheophytin; PQ/PQH_2, plastoquinone/plastoquinol; PSII, photosystem II; Q_A and Q_B, primary and secondary quinone electron acceptors, respectively; TR-MIMS, time-resolved membrane-inlet mass spectrometry.

REFERENCES

(1) Messinger, J., and Shevela, D. (2012) Principles of photosynthesis. In *Fundamentals of Materials and Energy and Environmental Sustainability* (Ginley, D., and Cachen, D., Eds.) pp 302−314, Cambridge University Press, Cambridge, U.K.

(2) Junge, W. (2019) Oxygenic photosynthesis: history, status and perspective. *Q. Rev. Biophys. 52*, e1.

(3) Kern, J., Chatterjee, R., Young, I. D., Fuller, F. D., Lassalle, L., Ibrahim, M., Gul, S., Fransson, T., Brewster, A. S., Alonso-Mori, R., Hussein, R., Zhang, M., Douthit, L., de Lichtenberg, C., Cheah, M. H., Shevela, D., Wersig, J., Seuffert, I., Sokaras, D., Pastor, E., Weninger, C., Kroll, T., Sierra, R. G., Aller, P., Butryn, A., Orville, A. M., Liang, M., Batyuk, A., Koglin, J. E., Carbajo, S., Boutet, S., Moriarty, N. W., Holton, J. M., Dobbek, H., Adams, P. D., Bergmann, U., Sauter, N. K., Zouni, A., Messinger, J., Yano, J., and Yachandra, V. K. (2018) Structures of the intermediates of Kok's photosynthetic water oxidation clock. *Nature 563*, 421−425.

(4) Cardona, T., Sedoud, A., Cox, N., and Rutherford, A. W. (2012) Charge separation in Photosystem II: A comparative and evolutionary overview. *Biochim. Biophys. Acta, Bioenerg. 1817*, 26−43.

(5) Shen, J.-R. (2015) The structure of photosystem II and the mechanism of water oxidation in photosynthesis. *Annu. Rev. Plant Biol. 66*, 23−48.

(6) Renger, G. (2012) Mechanism of light induced water splitting in Photosystem II of oxygen evolving photosynthetic organisms. *Biochim. Biophys. Acta, Bioenerg. 1817*, 1164−1176.

(7) Warburg, O., and Krippahl, G. (1958) Hill-Reaktionen. *Z. Naturforsch., B: J. Chem. Sci. 13*, 509−514.

(8) Shevela, D., Eaton-Rye, J. J., Shen, J.-R., and Govindjee (2012) Photosystem II and the unique role of bicarbonate: A historical perspective. *Biochim. Biophys. Acta, Bioenerg. 1817*, 1134−1151.

(9) McConnell, I. L., Eaton-Rye, J. J., and Van Rensen, J. J. S. (2012) Regulation of photosystem II electron transport by bicarbonate. In *Photosynthesis: Plastid Biology, Energy Conversion and Carbon Assimilation* (Eaton-Rye, J. J., Tripathy, B. C., and Sharkey, T. D., Eds.) pp 475−500, Springer, Dordrecht, The Netherlands.

(10) Aoyama, C., Suzuki, H., Sugiura, M., and Noguchi, T. (2008) Flash-induced FTIR difference spectroscopy shows no evidence for the structural coupling of bicarbonate to the oxygen-evolving Mn cluster in photosystem II. *Biochemistry 47*, 2760−2765.

(11) Shevela, D., Su, J. H., Klimov, V., and Messinger, J. (2008) Hydrogencarbonate is not a tightly bound constituent of the water-oxidizing complex in photosystem II. *Biochim. Biophys. Acta, Bioenerg. 1777*, 532−539.

(12) Ulas, G., Olack, G., and Brudvig, G. W. (2008) Evidence against bicarbonate bound in the O_2-evolving complex of photosystem II. *Biochemistry 47*, 3073−3075.

(13) Umena, Y., Kawakami, K., Shen, J.-R., and Kamiya, N. (2011) Crystal structure of oxygen-evolving photosystem II at a resolution of 1.9 Å. *Nature 473*, 55−60.

(14) Villarejo, A., Shutova, T., Moskvin, O., Forssen, M., Klimov, V. V., and Samuelsson, G. (2002) A photosystem II-associated carbonic anhydrase regulates the efficiency of photosynthetic oxygen evolution. *EMBO J. 21*, 1930−1938.

(15) Shutova, T., Kenneweg, H., Buchta, J., Nikitina, J., Terentyev, V., Chernyshov, S., Andersson, B., Allakhverdiev, S. I., Klimov, V. V., Dau, H., Junge, W., and Samuelsson, G. (2008) The photosystem II-associated Cah3 in *Chlamydomonas* enhances the O_2 evolution rate by proton removal. *EMBO J. 27*, 782−791.

(16) Shevela, D., Noring, B., Koroidov, S., Shutova, T., Samuelsson, G., and Messinger, J. (2013) Efficiency of photosynthetic water oxidation at ambient and depleted levels of inorganic carbon. *Photosynth. Res. 117*, 401−412.

(17) Ananyev, G., Nguyen, T., Putnam-Evans, C., and Dismukes, G. C. (2005) Mutagenesis of CP43-arginine-357 to serine reveals new evidence for (bi)carbonate functioning in the water oxidizing complex of photosystem II. *Photochem. Photobiol. Sci. 4*, 991−998.

(18) Koroidov, S., Shevela, D., Shutova, T., Samuelsson, G., and Messinger, J. (2014) Mobile hydrogen carbonate acts as proton acceptor in photosynthetic water oxidation. *Proc. Natl. Acad. Sci. U. S. A. 111*, 6299−6304.

(19) Banerjee, G., Ghosh, I., Kim, C. J., Debus, R. J., and Brudvig, G. W. (2019) Bicarbonate rescues damaged proton-transfer pathway in photosystem II. *Biochim. Biophys. Acta, Bioenerg. 1860*, 611−617.

(20) Wydrzynski, T., and Govindjee (1975) New site of bicarbonate effect in photosystem II of photosynthesis - Evidence from chlorophyll fluorescence transients in spinach-chloroplasts. *Biochim. Biophys. Acta, Bioenerg. 387*, 403−408.

(21) Vermaas, W. F. J., and Rutherford, A. W. (1984) EPR measurements of the effects of bicarbonate and triazine resistance on the acceptor side of photosystem II. *FEBS Lett. 175*, 243−248.

(22) Hienerwadel, R., and Berthomieu, C. (1995) Bicarbonate binding to the non-heme iron of photosystem II investigated by Fourier transform infrared difference spectroscopy and 13C-labeled bicarbonate. *Biochemistry 34*, 16288−16297.

(23) Ferreira, K. N., Iverson, T. M., Maghlaoui, K., Barber, J., and Iwata, S. (2004) Architecture of the photosynthetic oxygen-evolving center. *Science 303*, 1831−1838.

(24) Van Rensen, J. J. S., Tonk, W. J. M., and De Bruijn, S. M. (1988) Involvement of bicarbonate in the protonation of the secondary quinone electron acceptor of photosystem II *via* the non-heme iron of the quinone-iron acceptor complex. *FEBS Lett. 226*, 347−351.
(25) Sedoud, A., Kastner, L., Cox, N., El-Alaoui, S., Kirilovsky, D., and Rutherford, A. W. (2011) Effects of formate binding on the quinone-iron electron acceptor complex of photosystem II. *Biochim. Biophys. Acta, Bioenerg. 1807*, 216−226.
(26) Saito, K., Rutherford, A. W., and Ishikita, H. (2013) Mechanism of proton-coupled quinone reduction in photosystem II. *Proc. Natl. Acad. Sci. U. S. A. 110*, 954−959.
(27) Eaton-Rye, J. J., and Govindjee (1988) Electron transfer through the quinone acceptor complex of photosystem II in bicarbonate-depleted spinach thylakoid membranes as a function of actinic flash number and frequency. *Biochim. Biophys. Acta, Bioenerg. 935*, 237−247.
(28) Blubaugh, D. J., and Govindjee (1988) The molecular mechanism of the bicarbonate effect at the plastoquinone reductase site of photosynthesis. In *Molecular Biology of Photosynthesis* (Govindjee, Ed.) pp 441−484, Springer, Dordrecht, The Netherlands.
(29) Govindjee, Weger, H. G., Turpin, D. H., van Rensen, J. J. S., Devos, O. J., and Snel, J. F. H. (1991) Formate releases carbon dioxide/bicarbonate from thylakoid membranes - measurements by mass spectroscopy and infrared gas analyzer. *Naturwissenschaften 78*, 168−170.
(30) Govindjee, Xu, C., and van Rensen, J. J. S. (1997) On the requirement of bound bicarbonate for photosystem II activity. *Z. Naturforsch., C: J. Biosci. 52*, 24−32.
(31) Tikhonov, K., Shevela, D., Klimov, V. V., and Messinger, J. (2018) Quantification of bound bicarbonate in photosystem II. *Photosynthetica 56*, 210−216.
(32) Brinkert, K., De Causmaecker, S., Krieger-Liszkay, A., Fantuzzi, A., and Rutherford, A. W. (2016) Bicarbonate-induced redox tuning in Photosystem II for regulation and protection. *Proc. Natl. Acad. Sci. U. S. A. 113*, 12144−12149.
(33) Rutherford, A. W., Paterson, D. R., and Mullet, J. E. (1981) A light-induced spin-polarized triplet detected by EPR in Photosystem II reaction centers. *Biochim. Biophys. Acta, Bioenerg. 635*, 205−214.
(34) Rutherford, A. W., Osyczka, A., and Rappaport, F. (2012) Back-reactions, short-circuits, leaks and other energy wasteful reactions in biological electron transfer: Redox tuning to survive life in O_2. *FEBS Lett. 586*, 603−616.
(35) Roach, T., Sedoud, A., and Krieger-Liszkay, A. (2013) Acetate in mixotrophic growth medium affects photosystem II in *Chlamydomonas reinhardtii* and protects against photoinhibition. *Biochim. Biophys. Acta, Bioenerg. 1827*, 1183−1190.
(36) Messant, M., Timm, S., Fantuzzi, A., Weckwerth, W., Bauwe, H., Rutherford, A. W., and Krieger-Liszkay, A. (2018) Glycolate induces redox tuning of photosystem II *in vivo*: Study of a photorespiration mutant. *Plant Physiol. 177*, 1277−1285.
(37) Winget, G. D., Izawa, S., and Good, N. E. (1965) Stoichiometry of photophosphorylation. *Biochem. Biophys. Res. Commun. 21*, 438−441.
(38) Messinger, J., and Renger, G. (1993) Generation, oxidation by the oxidized form of the tyrosine of polypeptide D2, and possible electronic configuration of the redox States S_0, S_{-1} and S_{-2} of the water oxidase in isolated spinach thylakoids. *Biochemistry 32*, 9379−9386.
(39) Shevela, D., and Messinger, J. (2013) Studying the oxidation of water to molecular oxygen in photosynthetic and artificial systems by time-resolved membrane-inlet mass spectrometry. *Front. Plant Sci. 4*, 473.
(40) Shevela, D., Schröder, W. P., and Messinger, J. (2018) Liquid-Phase Measurements of Photosynthetic Oxygen Evolution. In *Photosynthesis: Methods and Protocols* (Covshoff, S., Ed.) pp 197−211, Springer, New York.
(41) Zimmermann, J.-L., and Rutherford, A. W. (1986) Photoreductant-induced oxidation of Fe^{2+} in the electron-acceptor complex of photosystem II. *Biochim. Biophys. Acta, Bioenerg. 851*, 416−423.
(42) Mende, D., and Wiessner, W. (1985) Bicarbonate *in vivo* requirement of photosystem II in the green alga *Chlamydobotrys stellata*. *J. Plant Physiol. 118*, 259−266.
(43) Carrieri, D., Ananyev, G., Brown, T., and Dismukes, G. C. (2007) *In vivo* bicarbonate requirement for water oxidation by photosystem II in the hypercarbonate-requiring cyanobacterium *Arthrospira maxima*. *J. Inorg. Biochem. 101*, 1865−1874.
(44) Ananyev, G., and Dismukes, G. C. (2005) How fast can photosystem II split water? Kinetic performance at high and low frequencies. *Photosynth. Res. 84*, 355−365.

https://dx.doi.org/10.1021/acs.biochem.0c00208
Biochemistry 2020, 59, 2442−2449